Geotech Geol Eng (2012) 30:1025–1034
DOI 10.1007/s10706-012-9524-3

ORIGINAL PAPER

Numerical Study of a Failure of a Reinforced Earth Retaining Wall

A. Sengupta

Received: 24 July 2008 / Accepted: 16 May 2012 / Published online: 25 May 2012

Abstract The case history of a failure of a RE wall has been presented. The wall failed immediately upon completion due to the overestimation of the strengths of the foundation clay layers and due to the underestimation of the self weight of the fill materials. A typical cross-section of the wall along with the stabilizing embankment and the foundation are modeled numerically by the limit equilibrium method and by a finite element method. The strengths of the foundation soils are determined by field tests done after the failure of the wall. Both the analyses predicted failure of the wall. The deformations predicted by the finite element method are found to be comparable to the observed field data. The numerical analyses further indicate that by consolidating a foundation clay layer to a minimum undrained strength of 45 kPa, the required factor of safety for the wall along with the road embankment can be achieved theoretically. Accordingly, prefabricated vertical drains are used to expedite the drainage and consolidation of the foundation clay layers. After the field tests confirm that the required minimum undrained strength is achieved, the RE wall and the embankment have been rebuilt successfully and now in full operation.

Keywords Reinforced earth retaining wall · Slope failure · Limit equilibrium analysis · Finite element analysis · Prefabricated vertical drain · Undrained strength

1 Introduction

A reinforced earth (RE) retaining wall supporting a 10.7-m high earthwork adjacent to a highway bridge on National Highway, NH-6 near Kolkata (India) developed a distress on the early morning of February 9, 2006. The affected bridge approach was opened to traffic about a month prior to the date of the incident. During this incident, a section of the newly constructed 4-lane approach vertically settled rapidly by about 3 m and laterally translated outwardly by about 1 m (see Fig. 1). The subsidence covered a width of about 60 % of the newly constructed bridge approach. Though the movement was relatively rapid initially, post failure records indicate that the structure continued to move for 9 days following the initial failure as is apparent from Fig. 2.

This paper presents the numerical analyses, including the traditional limit equilibrium slope stability analyses and the finite element analyses, performed during the investigation into the failure and to check the proposed remedial measure.

A. Sengupta (✉)
Department of Civil Engineering, Indian Institute of Technology, Kharagpur 721302, India
e-mail: sengupta@civil.iitkgp.ernet.in

Fig. 1 Failure of the RE wall (note the exposed portion of the concrete bridge and the remains of the RE wall)

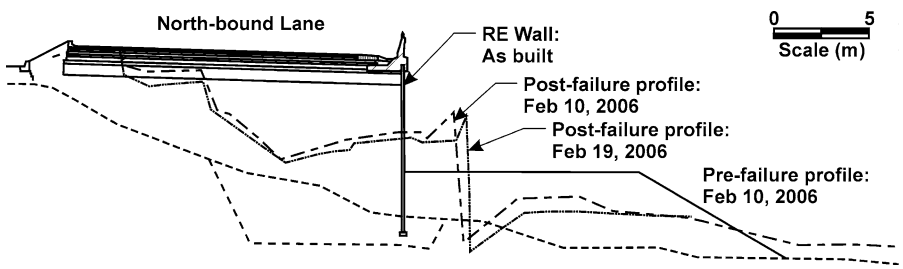

Fig. 2 Failed embankment cross section prior to and following the incident

2 Construction History of the Road Embankment

The original highway was a two lane undivided highway that was constructed about 30 years ago. This old earthen embankment had a side slope of 3 (horizontal) to 1 (vertical). In 2006, it was converted into a 4-lane highway by constructing a new embankment by the side of the old embankment. The land being waterlogged and marshy, it was first dewatered when the construction for the two additional lanes started in 2004. The top surface was stripped and a compacted layer of sand was placed. The RE wall construction began by the end of February 2004. The reinforced embankment was 8 m high by June 2004 and 9.25 m high in February 2005. There was a stop in work for a while in 2005. The construction again resumed in November 2005. The construction of the embankment was completed in December 2005. The road was open to traffic in January 2006 but the embankment collapsed on February 9, 2006.

3 The Subsurface Condition

The failed road embankment is located within the inter-tidal flats and back-swamps of the Hoogly River

a major tributary of the River Ganges. The local soil is mainly fine grained silts and clays of Iocene and Pleistocene age (Vaidyanadhan and Ghosh 1993).

The subsurface investigation undertaken after the incident included drilling of fourteen boreholes for conducting in situ tests (standard penetration and field vane shear tests) and obtaining soil samples for laboratory tests. The laboratory tests included unconsolidated undrained (UU) triaxial tests and one-dimensional incrementally loaded consolidation tests besides grain size distribution, natural water content and Atterberg limit tests of selected tube samples. The boreholes BL1, BL2, BL3 were drilled at Chainage 18.258 km outside of the outer face of the failed segment of the RE wall. Field vane shear tests were conducted at locations V1 and V3 along this Chainage outside the area of the embankment. Within the embankment area at Chainage 18.258, the boreholes BU1 and BU2 were drilled. Similarly BL4, BL5 and BL6 were drilled at Chainage 18.317 km outside of the embankment area, while BU3 and BU4 were drilled at this Chainage within the embankment area. Locations of these boreholes are shown on Fig. 3 along with the results of the topographic survey undertaken immediately after the incident. Three additional boreholes, BU5, BU6 and BU7 were drilled outside the failed section at Chainage 18.350 km.

Data from this investigation confirm that the site is located within the Holocene silty clay, which is underlain in turn by stiff silty clay presumably of Pleistocene age. The upper 5–8 m of the Holocene silty clay is of firm consistency and is lightly overconsolidated with a preconsolidation pressure of up to 200 kPa. Underneath this layer, a silty clay layer containing organics was found. Laboratory tests on soil sample obtained from this layer indicate that this normally to very lightly overconsolidated layer has a significantly higher compressibility than the overlying and underlying Holocene soil units. Underneath the silty clay layer containing organics, firm silty clay probably of Holocene age or stiff silty clay with sand or sandy silt partings of Pleistocene age is encountered. This layer is overconsolidated with a preconsolidation pressure of up to 300 kPa. The undrained shear strengths, s_u, obtained from laboratory unconsolidated undrained tests and field vane tests are plotted against the effective vertical stress, σ'_v, in Fig. 4. Little undrained shear strength data appears to

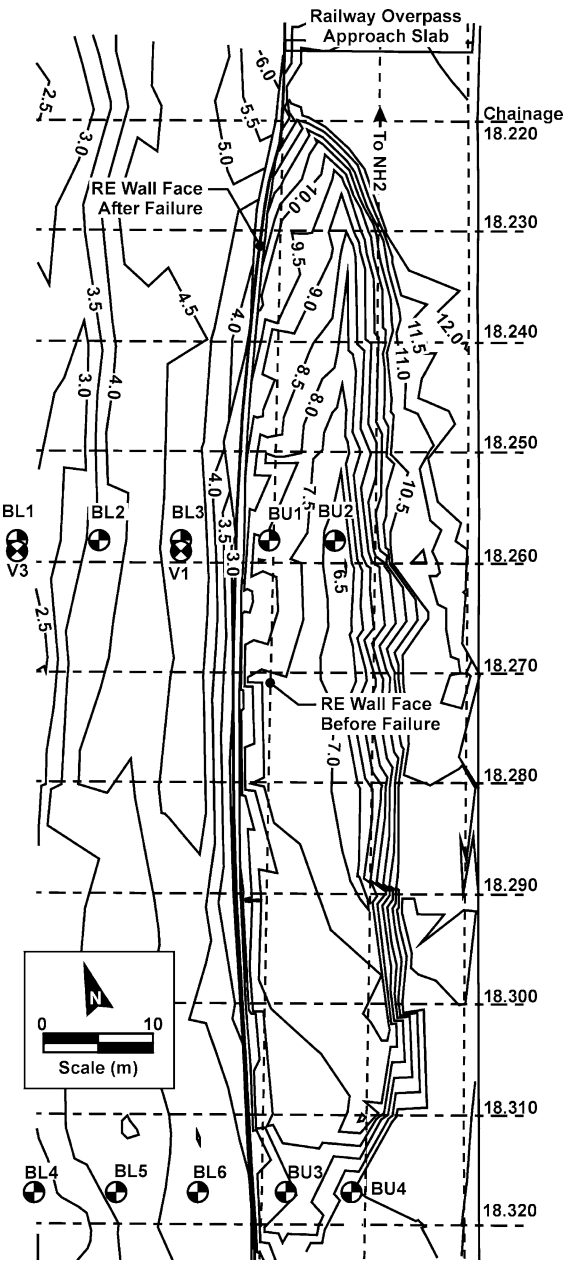

Fig. 3 Borehole locations

have been obtained from investigations conducted within or near the affected section of the embankment before the construction of the RE wall. Only two boreholes, BH5 and BH6, were drilled near the site prior to the construction of the RE wall. Four estimates of undrained shear strength obtained from the laboratory testing of samples extracted from these boreholes are of any relevance. These data, included in Fig. 4 for

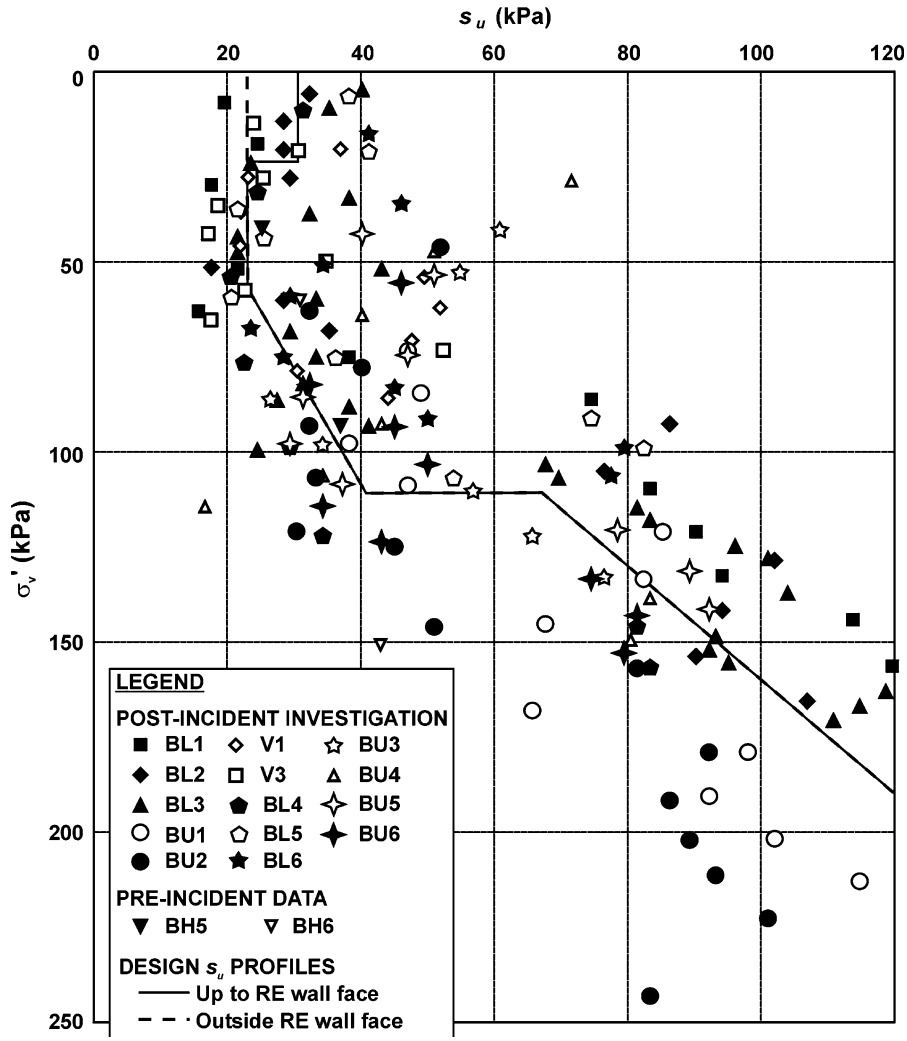

Fig. 4 Measured undrained shear strengths

comparison, do not appear to capture the soft nature of the near surface soils outside the toe of the RE wall.

One-dimensional incrementally loaded consolidation test data indicate that at the time of the failure, the soils were completely consolidated under the stresses imposed by the old embankment. In addition, the upper 2.5 m of the native soils also likely to have undergone 50 % consolidation under the newly constructed RE embankment and the stabilizing berm, while the deeper native soil layers did not consolidate appreciably under the imposed stresses.

4 Numerical Analyses of the Failure

The failure of the RE wall is studied numerically by modeling the wall along with the backfill and the stabilizing berm. Traditional limit equilibrium slope stability analyses as well as finite element analyses with soil-structure interaction capability are carried out to understand the failure mechanism. The material strength parameters utilized in the analyses are obtained from the laboratory and the field tests and are summarized in Table 1. The undrained shear strengths listed in the Table 1 are assumed according to the information presented in the Fig. 4. The variation of the undrained strength (s_u) for the soil type 4 is from 28 to 32 kPa with an average value of 23 kPa. For the soil type 3 under the embankment, the variation of the undrained strength is between 22 and 40 kPa with an average value of 30 kPa. Similarly, for soil types 5 and 6, the average values of undrained strength are 28 and 38 kPa, respectively. The shear strengths of the new and old embankment fills are

Table 1 Material strength parameters

Location	Soil unit*	Elevation (m) with respect to original ground surface		Total unit weight (kN/m^3)	Friction angle, ϕ'	Undrained strength, s_u (kPa)
		Top of layer	Bottom of layer			
Outside of embankment	4	0	−10	16.5	–	23
Underneath embankment	3	0	−4	16.0	–	30
	4	−4	−10	16.5	–	23
	5	−10	−12	17.0	–	28
	6	−12	−16	17.0	–	38
Old embankment	1	+8.0 (max)	0	18.0	35°	20
New embankment	2	+10.0 (max)	0	19.0	38°	–

Soil types 1 and 2 are old and new backfill (sand) materials. Soil types 3, 4, 5 and 6 are silty clay materials

Soil units are numbered as in Fig. 5

obtained from laboratory triaxial test data on undisturbed samples obtained by boring.

Figure 5 shows a typical cross section of the road embankment along with the foundation soil profiles at the failed section of the highway. The strength parameters of the different soil types shown in the figure are presented in Table 1.

4.1 Limit Equilibrium Stability Analysis of the Road Embankment

Using the shear strength parameters listed in Table 1, undrained stability of the RE wall is assessed for the RE wall configuration (refer to Fig. 5) at the time of the incident. A modified version of the limit equilibrium slope stability assessment computer program UTEXAS2 (Edris and Wright 1992) is used in this analysis. For computing the minimum factor of safety, the simplified Bishop method of analysis (Bishop 1955) was adopted. In the simplified Bishop's method, the interslice forces are assumed to be horizontal. The force equilibriums in both directions are not satisfied but the overall moment equilibrium is satisfied. A search is performed for a critical circular slip surface and the corresponding limit equilibrium factor of safety, *FS*. The results are presented in Fig. 6. These results indicate that the wall was indeed in a state of marginal stability.

The present limit equilibrium stability assessment indicates that the original RE wall would have been at a state of instability with a static factor of safety of 0.983 at the time of failure. The original design indicated a limit equilibrium factor of safety against bottom rotational failure under static condition of 1.42. Major reasons for the lack of agreement between the present analyses and those carried out during the original design of the embankment appear to be due to change in geometry of the wall and change in fill material properties. The maximum height of the embankment was about 9.6 m. How ever, the original RE wall design called for 7.2 m of embankment height plus a surcharge that approximately translates to about additional 1 m of embankment height, that is, a total height of embankment of about 8.2 m. Because of the intended use of fly ash in embankment construction, in the original RE wall design, a unit weight of 16 kN/m^3 was assumed for the fill material. Since the embankment behind the RE wall was ultimately constructed with river sand, the unit weight assumed during the original design turned out to be smaller than the actual.

4.2 Finite Element Analysis of the RE Wall and the Embankment

The finite element analysis of the pre-failure geometry of the RE wall is performed using a modified version of the finite element program "Soilstruc" originally developed by Clough and Duncan (1969). In the used version of the program, the undrained behaviors of clays are modeled as Von Mises type of materials with bilinear stress–strain curves. The material model required the unit weight, elastic modulus (E), Poisson's ratio (ν), friction angle, (ϕ) and the undrained cohesion, (c_u) to be specified. Both the walls are modeled by beam elements. Interface elements are

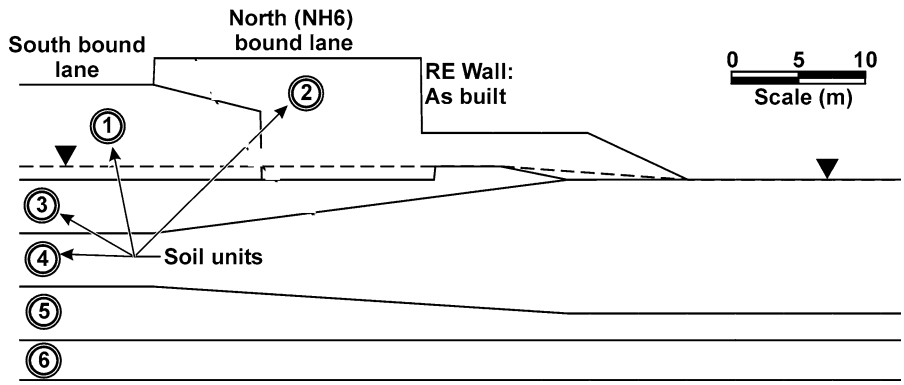

Fig. 5 A typical pre-failure RE wall cross section

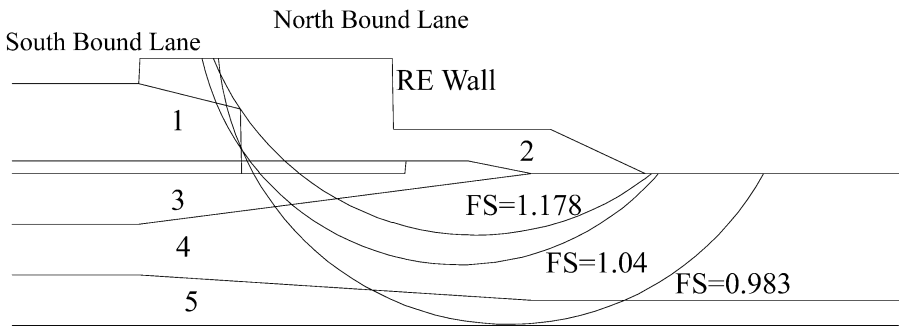

Fig. 6 Results of limit equilibrium stability assessment of the RE wall

introduced between the wall and the backfill soil elements. The additional material parameters like elastic modulus, Poisson's ratio, interface friction (δ), etc., assumed in the finite element analysis for the in situ soils and backfill soils are listed in Table 2. The soil types 1, 3, 4, 5 and 6 are assumed to be in undrained condition. Thus Poisson's ratio for these soils is set to be close to 0.5. The newly placed sand fill material (soil type 1) is modeled as drained material with the phreatic surface specified as shown in Fig. 5. In absence of proper test data, the modulus values of soils are estimated from the literature and the past experience. The modulus value of the concrete wall is obtained using the expression, $E = 5{,}000*(f_{ck})^{1/2}$ where f_{ck} is the characteristic cube compressive strength of concrete and equal to 20 N/mm^2 for a M20 grade concrete (BIS 2000). The interface friction between the sand backfill and concrete wall is taken as 75 % of the friction angle of the sand fill (Gireesha and Muthukkumaran 2011).

The finite element model of the walls and the road embankment consists of 394 nodes, 356 soil elements, 65 structural elements and 10 special (interface) elements. Figure 7 shows the discretization of the wall, its backfill and the foundation. The construction of the road embankment is modeled in 10 equal steps (lifts).

The finite element results at the end of construction in terms of deformations and velocity vectors are shown graphically in Figs. 8 and 9, respectively. The numerical analyses predict failure due to excessive deformations in the backfill soil adjacent to the retaining walls. The failure predicted by the numerical model is comparable with the failure observed in the reality. Table 3 compares deformations of the retaining walls predicted by the analysis with those observed in the actual field.

The settlements and lateral shift of the roadway adjacent to the retaining wall obtained from the numerical analysis are comparable with those observed and recorded in the actual field. The minimum factor of safety for slope stability is found to be 0.51 for shallow surface near the retaining wall and 1.04 for a deep seated slip surface. The minimum factor of safety for the deep seated critical slip circle is found to be 0.983 by the limit equilibrium slope stability analysis.

Table 2 Material parameters for the FEM study

Material	Unit weight (kN/m^3)	Young's modulus, E (kPa)	Poisson's ratio, ν	Friction angle, ϕ, in degree	Undrained cohesion, c_u (kPa)
Soil 1	18.0	50,000.0	0.49	35	20.0
Soil 2	19.0	10,000.0	0.30	38	0.0
Soil 3	16.0	25,000.0	0.49	0	30.0
Soil 4	17.0	32,000.0	0.49	0	23.0
Soil 5	17.0	35,000.0	0.49	0	28.0
Soil 6	19.0	60,000.0	0.49	0	38.0
Wall	23.5	22,360,680	0.20		
Interface between soil and wall				28	

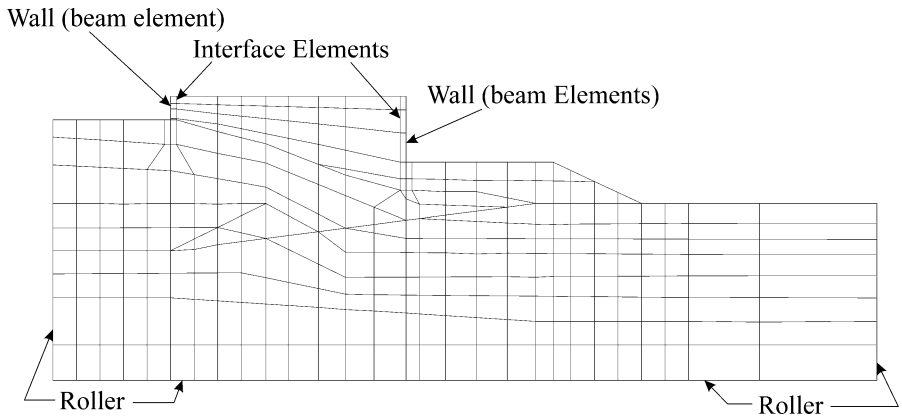

Fig. 7 Finite element discretization of the wall, berm and foundation soils

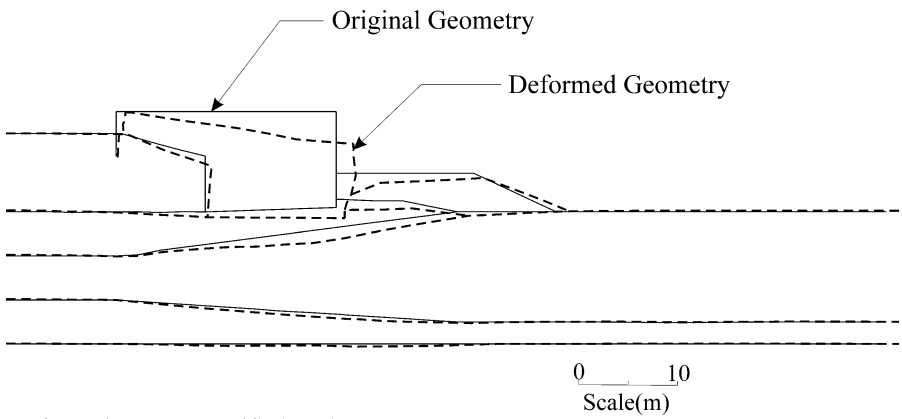

Deformations are magnified 10 times

Fig. 8 Deformed geometry as obtained from the finite element analysis

5 Reconstruction of the RE Wall

Several reconstruction alternatives are reviewed for the failed RE wall. These include installing bored piles along the outer edge of the stabilizing berm that runs along the failed RE wall. The option of reconstruction of the embankment with light weight fill, that is, expanded polystyrene (EPS) and foam concrete is also considered. The other possible remedial measure explored is the installation of prefabricated vertical drains (PVDs) to drain and consolidate the foundation clays. Based on the economic considerations, ease of

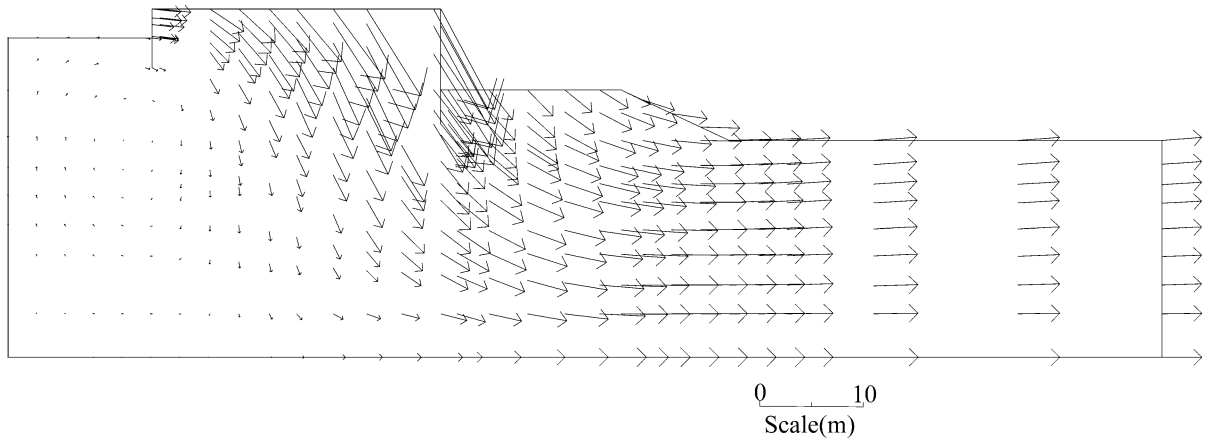

Fig. 9 Velocity vectors as computed in the finite element analysis

Table 3 Comparison of the results of the numerical analyses with field data

Field observations		Results of limit equilibrium analysis	Results of the present finite element analysis		
Vertical settlement of road	Lateral shift of the retaining wall	Minimum factor of safety	Vertical settlement of the road	Lateral shift of the wall	Minimum factor of safety
3 m	1 m	0.983	2.2 m	1.2 m	0.51

construction, availability of construction materials, etc., the last option is chosen. The numerical analyses are repeated to find out the required undrained strengths of the foundation soils to stabilize the RE walls. Figure 10 shows that based on limit equilibrium analyses, if the foundation soil type 4, has a minimum undrained strength of 45 kPa, (keeping strengths for all other soils same as before) the required minimum factor of safety of 1.2 shall be met for the embankment stability. Therefore attempts are made to drain and consolidate the soil types 4 and 5 under the road embankment with PVDs to achieve the above required minimum undrained strength. The method included installation of PVDs up to 13 m depth, construction of a two-stepped stabilizing berm along the outer face of the failed wall, and reconstruction of the RE wall and the highway embankment.

The PVDs (Colbondrain® CX 1000) were installed in October 2006 at 1.2 m horizontal spacing in a square grid pattern using a mandrel of diamond shaped cross section with diagonals measuring 50 and 120 mm. The width of the PVD treated zone was 19 m measured from the face of the failed wall. The stabilizing berm was constructed between October 2006 and February 2007. The height of the upper bench was 3 m lower than the finished road grade and its width was 20 m. The maximum overall berm width measured from the base of the reconstructed RE wall to the toe of the lower bench was 37 m. After removing the failed embankment to an elevation of about 5.75 m above the original ground surface, reconstruction work for the RE wall was taken up in February 2007. Drilling, sampling and Standard Penetration Testing and field vane shear tests were conducted at the end of April 2007 to check whether the gain in undrained shear strength due to accelerated consolidation of soft soils within the PVD treated zone met the required value. Data from these tests, presented in Fig. 11 together with the undrained shear strengths from nearby locations measured immediately after failure, indicate that the increased undrained shear strengths, following accelerated consolidation of the soils within the PVD treated zone for the most part, exceeded those assumed in the overall stability assessment for the embankment redesign. Embankment reconstruction above 8 m height was allowed from May 2007 after these data were reviewed. Fill placement for the remaining height continued thereafter and paving work was completed by the beginning of June 2007. The reconstructed

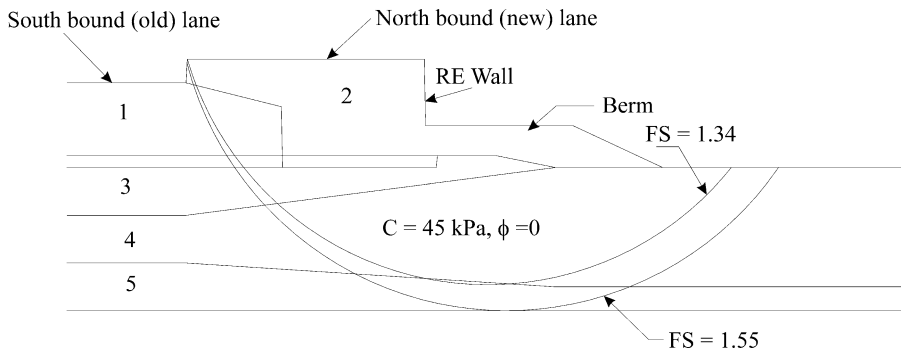

Fig. 10 Stability assessment of the RE wall with undrained strength of 45 kPa for foundation soil type 4

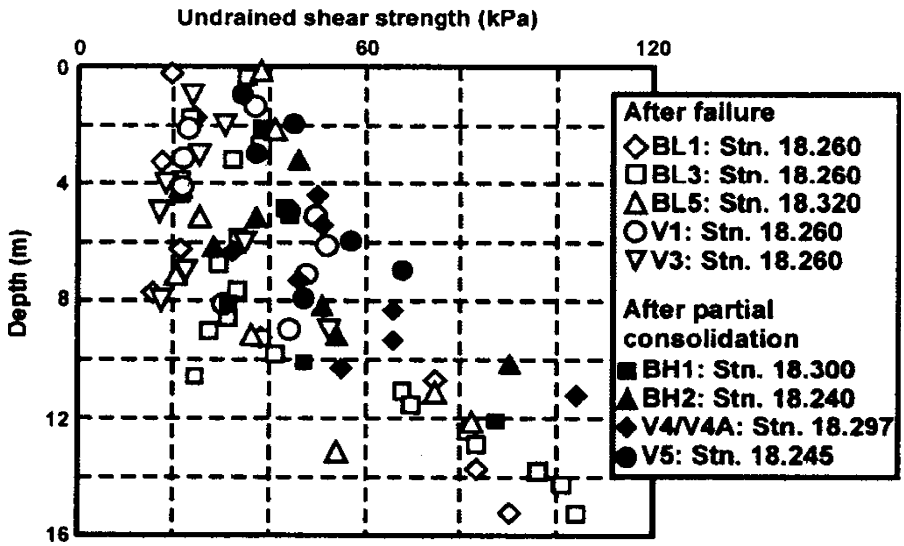

Fig. 11 Consolidation related increase in undrained shear strength after installation of PVDs

highway embankment was reopened for vehicular traffic by the middle of June 2007. Since then the RE wall is performing satisfactorily.

6 Conclusions

The case history of a failure of a RE wall has been presented. The failure is modeled numerically by limit equilibrium method and by finite element method. Both the methods of analysis predicted the failure. The deformations predicted by the finite element method are found to be comparable to the observed field data. The failure of the wall and the embankment immediately upon construction is found to be due to the overestimation of the strengths of the foundation clay layers and due to the underestimation of the self weight of the fill materials. This kind of failures is becoming more and more common at least in this part of the world as to meet the fast growing economy, infrastructures like roads are being built at a very fast rate without paying adequate attention to the proper field investigation and determination of in situ strengths of the sub-soils. In this particular case, the failure of the retaining wall could have been avoided by slowing down the construction procedure giving the clay layers below the foundation enough time to consolidate and gain in strength and/or providing adequate drainage facility to the sub-soils to dissipate pore water pressure and to consolidate at a faster rate. In the present case, the performance of the prefabricated vertical drains (PVDs) are found to be excellent in expediting the drainage and consolidation of the foundation clay layers.

References

Bishop AW (1955) The use of slip circle in stability analysis of slopes. Geotechnique 5:7–17

Bureau of Indian Standards (2000) Indian standard plain and reinforced concrete—code of practice. IS456, 4th Revision, New Delhi, India

Clough GW, Duncan JM (1969) Finite element analysis of Port Allen and Old River Locks. Report No. TE 69-3, College of Engineering, Office of Research Services, University of California, Berkeley, CA

Edris EV, Wright SG (1992) UTEXAS2, Slope stability package, instruction report. GL-87-1, Department of the Army, U.S. Army Corps of Engineers, Washington, DC, Contract No. DACW39-89-C-0024

Gireesha NT, Muthukkumaran K (2011) Study on soil structure interface strength property. Int J Earth Sci Eng 4(6):89–93

Vaidyanadhan R, Ghosh RN (1993) Quaternary of the east coast of India. Curr Sci Indian Acad Sci 64:804–816